

LASER INTERFEROMETER GRAVITATIONAL WAVE OBSERVATORY  
-LIGO-  
CALIFORNIA INSTITUTE OF TECHNOLOGY  
MASSACHUSETTS INSTITUTE OF TECHNOLOGY

|  |
|--|
| <b>Technical Note</b> <b>LIGO-T000055- 00- R</b> 1/10/2000                       |
| <b>Proposal for upgrade of 40m prototype</b><br>Largeseismic stacks, and bakeout |
| D. Ugolini, S. Vass, A. Weinstein  |

This is an internal working note  
of the LIGO Project.

**California Institute of Technology**  
**LIGO Project - MS 18-34**  
**Pasadena CA 91125**  
Phone (626) 395-2129  
Fax (626) 304-9834  
E-mail: info@ligo.caltech.edu

**Massachusetts Institute of Technology**  
**LIGO Project - MS NW17-161**  
**Cambridge, MA 02139**  
Phone (617) 253-4824  
Fax (617) 253-4824  
E-mail: info@ligo.mit.edu

WWW: <http://www.ligo.caltech.edu/>

# Proposal for upgrade of 40m prototype seismic stacks, and bakeout

## Abstract

In preparation for upgrading the Caltech 40m interferometer for prototyping LIGO II optical configurations, we are considering the rebuilding of the existing 40m seismic stacks, and baking out the entire vacuum system. The various options, considerations, and pros and cons are discussed herein.

## 1 Introduction

The Caltech 40m interferometer is being upgraded in order to prototype advanced optical configurations appropriate for LIGO II operation (as discussed elsewhere). Before a new interferometer is installed, it may be necessary or desirable to make major modifications to the existing facility. The big projects that must be completed early on include:

- modifications to the existing building (repairing the roof, repairing the cranes, removing the wall separating the IFO hall from the current operations room, converting the north annex building to a new operations room, extensive electrical work, *etc.*);
- a new, EPICS-based vacuum control system, with (minor) upgrades to the vacuum hardware;
- the addition of a new output chamber with a new seismic stack;
- rebuilding the six existing seismic stacks, replacing the viton elastomer springs with LIGO-I damped metal springs;
- baking out the entire existing vacuum envelope.

The first three items listed above are more-or-less necessary, and non-controversial. The new EPICS-based vacuum control system is discussed in a companion document, which should be carefully reviewed.

The necessity for rebuilding of the six existing seismic stacks and baking out the vacuum envelope is by no means clear, as there are various pros and cons, based on many uncertainties. The purpose of this document is to present the relevant considerations, and solicit advice and recommendations as to the best course of action.

## 2 Overview

### 2.1 The currently existing stacks

At present, the 40m lab contains five seismic stacks with three legs and four stages, for the chambers housing the beam splitter (BS), south vertex (SV) test mass, south end (SE), east vertex (EV), and east end (EE). There is also an input optics chamber with a square optical table sitting on a one-leg, four stage stack. The layout can be seen in [1].

The three-legged stacks were installed in 4/93. The input optics chamber stack was built in 1996, and installed at the end of that year[2] Engineering drawings for these stacks exist [3].

In each of these stacks, the masses are machined stainless steel, and the springs are viton elastomer.

### 2.2 Upgrade to damped metal springs?

An engineering study of alternative spring designs was performed by HYTEC in 1996 [4]. In 1997, it was decided [5] that LIGO would use newly designed damped metal springs (with fluorel seats) in place of the viton elastomer, mainly for performance reasons, but also because of concerns about fluorocarbon contamination from the viton.

In the planning for the 40m upgrade for prototyping of advanced optical configurations, it was suggested that the stacks be rebuilt for the same reasons.

In preparation for such a rebuild, a (relatively simple) design analysis was performed (and documented in an appendix to this note). Based on this, sets of damped metal springs (500 non-epoxy springs, half left-handed and half right-handed, with Fluorel seats) were ordered. As we will see below, some 362 springs are needed for five 3-legged stacks and two one-legged stacks). Despite the destruction of the cleaning facility in Oklahoma by a hurricane, the cleaned Fluorel seats are now on hand, but the springs should arrive in a few months.

However, the case for such a rebuild is not uncontroversial, as discussed in the following sections.

### 2.3 Re-machining of the stack masses

Replacing the viton with damped metal springs in the existing seismic stack would of course require that the stacks be disassembled and then reassembled.

In addition, the viton springs are set in the stack masses inside of machined circular indentations, of diameter 6.35 cm (2.5 in) and depth 4.34 cm (1.71 in). The damped metal springs used at LIGO, in their Fluorel seats, have diameter 7.11 cm (2.80 in). Therefore, the indentations would have to be re-machined to accomodate the Fluorel seats. Then, all pieces (table, masses, springs and Fluorel seats) would have to be cleaned for vacuum use.

The metal springs and Fluorel seats have already been cleaned. However, as discussed below, the Fluorel seats would need to be flushed and then pressure-cooked with de-ionized water to minimize the fluorocarbon outgassing. At the same time, it would be prudent to pressure-cook all existing viton, including all the O-rings in the system.

### 2.4 Output chamber stack

In order to prototype RSE at the 40m, we will need to place a signal recycling mirror around one meter from the beam splitter at the dark port, thus necessitating an output vacuum chamber. The

chamber itself already exists, and is identical to the existing input chamber. However, no seismic stack was built for it.

We propose that we build such a stack, which can be nearly identical to the one-legged stack built for the input chamber. There are some 100 spare viton springs which can be used for this new stack, or we can use the damped metal springs that were ordered for the rebuild of the existing six stacks (sufficient quantities for all seven stacks were ordered).

We would proceed with this, independent of any decision on the rebuild of the existing stacks. Presumably, the output chamber would have to be baked out, in any case.

## 2.5 Performance versus contamination

The primary goal of the upgrade, prototyping advanced optical configurations, focusses on the shot-noise limited region of the LIGO band (above a few hundred Hz), and thus we are less concerned with the performance of the IFO in the region where seismic noise dominates (below 100 Hz).

As discussed below, the replacement of the viton springs with damped metal springs in the existing 40m stacks will provide superior isolation in the “signal” frequency band between 40 Hz and 100 Hz, but potentially much poorer performance in the “control” frequency band between 1 Hz and 20 Hz.

Since performance in the “signal” frequency band is of lesser importance for the primary goal of the upgrade, the main argument for rebuilding the stacks has been to potentially reduce the contamination of the optical elements from fluorocarbons originating in the viton springs.

## 3 Contamination

In the years 1997 through 1999, much effort went into bringing the 40m IFO into full lock in its “Mark 3” configuration (power-recycled recombined Michaelson with Fabry-Perot arms). This effort was never entirely successful.

Several measurements indicated that both 40m arms and recycling cavity had anomalously high losses, so that the IFO was distinctly undercoupled (as opposed to the overcoupled design). This produced a variety of problems, so that it was never possible to bring the IFO into full, stable lock with both arms aligned (at least, not without some trickery).

There was clear evidence of glint from a “spot” on the south end mass with extremely anomalous loss/scattering. This mass was removed on 1/10/2000 and inspected under the microscope in the OTF. It was easy to find a 3mm long, horizontal scratch, located slightly above center of the surface. This location is identical with the highly scattering horizontal line that had been observed under resonant conditions.

In addition, there is evidence (from several ring-down measurements made in the last several years) of anomalous losses ( $> 100$  ppm/mirror) on the mirror surfaces, which may have been growing with time.

It would be useful to correlate these losses with observed contamination on the mirror surfaces, but this does not seem possible with an optical microscope, and we know of no quick way to make such a measurement.

### 3.1 RGA scans

Fluorocarbons are present in the RGA scans of the residual gas in the 40m vacuum chamber, throughout the period (see Fig. 1). There is a clear peak at AMU 69 ( $\text{CF}_3$ ). The likely source of

these fluorocarbons are the viton springs in the seismic stacks.

Fluorocarbons react with residual water vapor to form hydrogen fluoride, which can etch glass and thus produce anomalous absorption and scattering losses.

This effect can be minimized by flushing and pressure-cooking the source of fluorocarbons with de-ionized water, which suppresses the outgassing of fluorocarbons.

### 3.2 Rebuild and bake-out

Under the assumption that the viton springs are the source of the fluorocarbons in the vacuum chamber, and are ultimately the source of the losses in the IFO cavities, we would want to replace them with springs containing less fluorocarbon material, and remove them from the vacuum walls with a bake-out.

### 3.3 Contamination from damped metal springs

Replacing the viton springs with damped metal springs will not eliminate fluorocarbons. The damped metal springs require Fluorel seats (Fluorel is the brand name of an elastomer similar or identical to Viton).

There would be lots of Fluorel in the system. According to Bill Althouse, the surface area of Fluorel in the seats is as large as the surface area of the viton it would replace; however, the volume of elastomer would be much reduced.

Is the level of fluorocarbons in the vacuum chamber governed by elastomer surface area or volume? For high concentrations, at the beginning of the high vacuum period, the decay of the fluorocarbon contribution is probably a surface-area effect; at lower concentrations, it is probably dominated by volume effects. It is not clear whether this level of fluorocarbon sourcing is troublesome.

### 3.4 Optical contamination

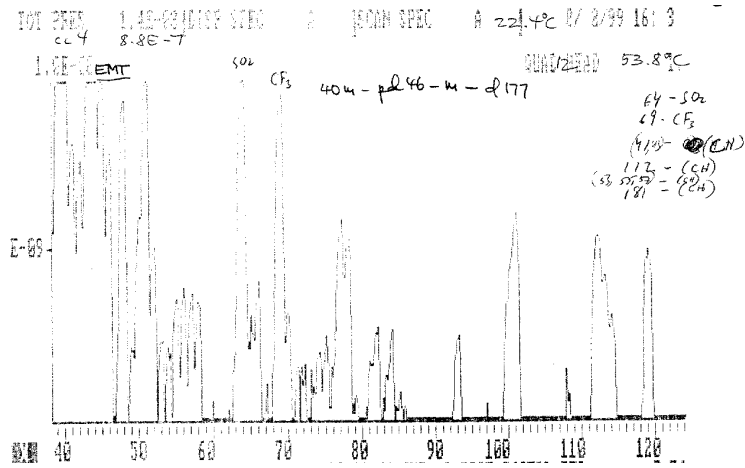
The effect of fluorocarbon contamination on a high-finesse optical cavity (with argon-ion laser light) was studied in [6], where they concluded that the degradation of mirror reflectivities due to Fluorel samples was less than 0.35 ppm/week, well within LIGO tolerances. It may be that the effect of fluorocarbons in the vacuum chamber is more of a catastrophic effect (etching of pits in only some cases), as opposed to a gradual effect on all mirrors.

In addition to fluorocarbons, hydrocarbons in the 40m vacuum chamber may be a source of concern for IFO operation. Hydrocarbons can be deposited on the optical surfaces, and burned on (“cracked”) by the high-powered laser, leading to absorption and scattering losses.

Optical contamination tests were performed by Jordan Camp and Daqun Li[7] in 1999, in which they measured the total and absorption losses via F-P cavity ringdown measurements with 1064 nm laser light, in the presence of a variety of materials which can outgas hydrocarbons. They found no evidence for gradual optical degradation from hydrocarbon cracking.

They concluded that the hydrocarbon cracking is not a problem at LIGO, or at the 40m upgrade, because of the change from green to IR (1064 nm) laser light; the cracking should be a strong function of the photon energy in this energy regime.

These observations suggest that a rebuild of the stacks in order to reduce hydrocarbon contamination of the optics may be unnecessary.



MARK II RGA SUM AMU DATA

Sum mass = AMU's 41,43,53,55,57

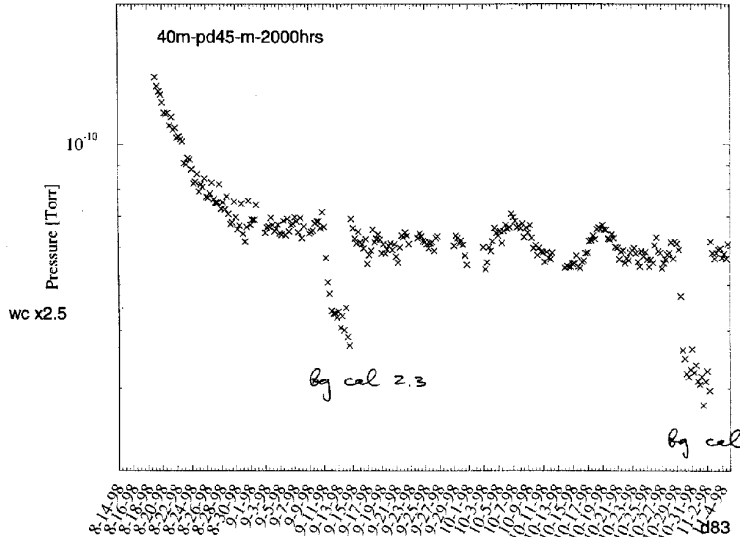


Figure 1: RGA measurements from the 40m vacuum system. Top: RGA scan from 8/99 has evident hydrocarbon peaks (AMUs in the range from 40 to 120),  $\text{SO}_2$  peak at 64, and  $\text{CF}_3$  at 69. The vertical scale has been enhanced (electron multiplication on). Bottom: History of partial pressure of AMU = 41,43,53,55,57 over 3 months in 1998.

### 3.5 Is a bake-out desired?

If the existing seismic stacks are removed and rebuilt, it would be a unique window for baking out the entire vacuum system. The hope would be that any remaining fluorocarbons attached to the walls and floors of the beam tubes and vacuum chambers could be eliminated.

As for the overall vacuum level: after some days of pump-down, the overall pressure (dominated by H<sub>2</sub>O, N<sub>2</sub>, and O<sub>2</sub>) is typically  $2 \times 10^{-6}$  torr. The contribution from hydrocarbons in the with masses of 41, 43, 53, 55, 57 is below  $10^{-10}$  torr. Nevertheless, it may be desirable to bake out the vacuum system, in an attempt to improve this further.

Note that if the stacks are *not* removed, it may make little sense to bake out the system (although the new output chamber still requires a bake-out). If the viton springs would continue to be employed, they would remain a large reservoir of fluorocarbons.

In order to do an effective bake out, all surfaces of the vacuum envelope would need to be heated, including the bottoms of the chambers. Since these lie close to the floor, the chambers must be jacked up so that heating jackets can be inserted between the chambers and the floor. This would not be practical unless the stacks are removed from the chambers.

We conclude that if the stacks are removed and rebuilt, it makes sense to bake out the entire vacuum envelope (even if you don't believe that hydrocarbons and fluorocarbons are a threat to the optical performance, it can't hurt to bake out); else, not.

### 3.6 The bake-out job

A bake-out of the 40m vacuum envelope is a big job; this was to be handled by Bill Althouse, but he has left us. It is important to have a qualified, experienced engineer handle such a task. Is one available?

One would have to:

- disassemble all seismic stacks.
- install the output chamber, stackless.
- jack up all the chambers.
- purchase and install heater pads under the chambers.
- get heater jackets for chambers and pipes, from LHO/LLO.
- electrical work for heaters.
- We may need an additional cryopump to handle the H<sub>2</sub>O load.
- We may need a new RGA with improved sensitivity.
- bake under vacuum, continuous monitoring, for weeks.
- Purchase and install a new, clean, hydrocarbon/fluorocarbon free air purge system to maintain the cleanliness of the vacuum envelope.

## 4 Performance

The damped metal springs are much less stiff (have a smaller spring constant) than the viton elastomer, for a given load-bearing ability; thus, they have superior high-frequency isolation. This feature comes at a price: they are much less well damped, so that motion at the top of the stack is worse at the normal mode frequencies of the stack.

### 4.1 Seismic wall position

The studies of the vertical transfer function  $T_{zz}$  discussed below suggest that the seismic wall improves from  $\sim 90\text{Hz}$  to  $\sim 40\text{Hz}$ . Since the goals of the upgrade focus on the frequency band above several hundred Hz, this gain may not seem particularly important. However, it is quite possible that interest may later focus on the thermal noise at the 40m, so that exposing more of it will be of great utility.

### 4.2 Suspension resonances

We plan on using core optics suspensions that are very similar to those used in LIGO-I; either scaled up SOS suspensions (scaling up from 3" to 4" optics), or scaled down LOS suspensions (from 10" to 4" optics). The LIGO-I SOS suspensions are bolted together, while the LOS suspensions are welded, so as to increase the frequency of the lowest mechanical resonance well above the seismic wall (*i.e.*, in the 150 Hz range).

If the seismic wall is moved from 100 Hz to 40 Hz, then there is no worry that seismic motion will excite mechanical resonances in the suspension frame. If, however, the seismic wall remains in the 100 Hz region, this *may* be a concern.

### 4.3 Damping

The four stages of masses and springs in these stacks result in four normal modes of vibration. At the frequencies of these normal modes, ground motion can be amplified, not suppressed. the degree to which the motion is amplified is determined by the damping (energy dissipation in the springs).

The metal springs are rather poorly damped. the internal viscoelastic layers provide a loss factor  $\eta$  of around 2 or 3%. The Fluorel seats, in addition to eliminating mechanical stresses due to the metal springs scraping against the metal stack masses, increase this to around 4% (*i.e.*, a  $Q$  of around 25). This is in contrast to the considerable damping afforded by the viton springs, with a lost factor of around 33%, or a  $Q$  of 3. (The complex (axial) spring constant is written  $k = Re(k)(1 + i\eta)$ , with  $\eta = 1/Q$ . In general, both  $Re(k)$  and  $\eta$  can be functions of frequency.)

### 4.4 The control band

The total (rms) differential seismic motion of the mirrors is suppressed using the standard ASC and LSC feedback loops, which operate over a broad range of frequencies (the "control" band).

The less stiff metal springs result in lower frequencies for the normal modes of the stacks (1-10 Hz for the vertical modes, as opposed to 10-20 Hz). The combination of low resonant frequency and poor damping means that the stacks employing damped metal springs have considerable motion in the frequency regime which, while far below the signal band of 100 Hz and above, is smack in the control band where the feedback loops must operate to keep the IFO in lock. Excessive motion here can have two negative effects:

- excessive displacement in any of the three dimensions (as measured by, eg,  $z_{rms}$ )

$$z_{rms}^2 \equiv \int_{f_{min}}^{\infty} z^2(f)df = \int_{f_{min}}^{\infty} z^2(f)f d(\log_{10} f)$$

may exceed the dynamic range of the control system;

- excessive velocity (as measured by  $v_{rms}$ )

$$v_{rms}^2 \equiv \int_{f_{min}}^{\infty} z^2(f)(2\pi f)df = \int_{f_{min}}^{\infty} z^2(f)(2\pi f^2)d(\log_{10} f)$$

may make it more difficult for the control system to grab and hold the mirror (bring it into lock).

Thus, the distinct advantages of the damped metal springs at signal frequencies may be more than offset by the inability to control the mirrors at the lower frequencies at which the stack likes to vibrate.

More relevant than  $z_{rms}$  and  $v_{rms}$  is the motion in the longitudinal direction (along the laser beam) and in the angular motion; but the simple modelling presented here models only vertical motion. Still, it is assumed that a comparison of the vertical motion between stacks composed of different springs is a useful figure of merit. See the next section.

#### 4.5 The transfer function

To quantify these issues at some level, we have made simple Matlab models of the vertical transfer function

$$T_{zz}(f) = \frac{x_{top}(f)}{x_{floor}(f)}$$

for stacks consisting of all viton springs, all damped metal springs, and mixtures of springs. Folding these in with the ground motion spectrum  $z_{floor}(f)$  allows us to predict the spectrum of motion at the top of the stack,  $z_{top}(f)$ , and calculate the integrated rms motion  $x_{rms}$  and  $v_{z,rms}$ .

#### 4.6 $T_{zz}$ versus $T_{xz}$ and $T_{xx}$

For IFO locking and noise performance, the relevant motion is in the direction along the beam ( $x$ ). However, the stacks are arranged vertically in the local gravitational field, and it is therefore easiest to model the vertical transfer function. The more relevant  $T_{zx}$  and  $T_{xx}$  transfer functions can only be reliably estimated using 3D finite element analysis tools, which take into account the more complex couplings of  $z$  to  $x$ , and all the complex properties of all the materials, their shear moduli and geometry, etc.

Fortunately, much work has already been done in this area, by Joe Giaime and others [8]. As summarized in Fig. 2, we see that:

- $T_{xz}$  and  $T_{xx}$  have seismic walls at frequencies typically a factor of 2 or more smaller than  $T_{zz}$ ;
- If  $T_{zz}$  has a peak at 9 Hz,  $T_{xz}$  and  $T_{xx}$  peak in the 2 to 3 Hz region, and otherwise lie below  $T_{zz}$ .
- These predictions were confirmed (qualitatively) with measurements of a test stack at MIT [8].

This figure can be used to qualitatively extrapolate from a model of  $T_{zz}$  to the more relevant  $T_{xz}$  and  $T_{xx}$ .

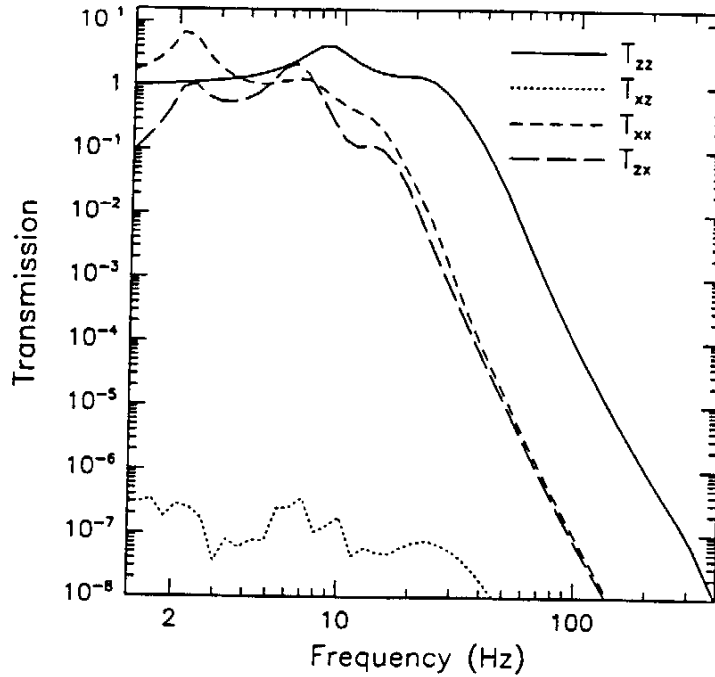


Figure 2: Transfer functions as modelled by symmetric ABAQUS model, of a viton stack similar to the 40m. From [8].

## 5 Seismic stack design

- I crudely estimate the masses of the stack, from dimensions found on drawings, using the density of steel:  $7.83 \text{ gm/cm}^3$ , for everything except for the Aluminum the top optical table of the three-legged stacks. Top Al optical table: 175 kg plus 50 kg payload; each leg mass: 92 kg. These will of course be measured carefully when we disassemble.
- The damped metal springs can support a maximum load of 100 lbs or 45 kg [4]. We put in as many springs as we need to hold the weight, and no more, thus minimizing the resonant frequencies. This translates to the following numbers of springs for each stage of the 3 legs, from top to bottom (so multiply by 3 to get the total per stage): 2,4,6,8. Total: 60 springs per stack.
- The spring constant for the damped metal springs at 100 Hz is  $k = 379 \text{ lbs/in}$ , or  $67.7 \text{ kg/cm}$  [4].
- The resonant frequency for stage  $i$ , in Hz, is  $f_i = \sqrt{N_{springs} N_{legs} k g / M} / (2\pi)$  where  $g =$  acceleration due to gravity. It's a coupled system, and a simple normal-mode analysis yields resonant frequencies for the stages from top to bottom: 3.6, 8.3, 13.0, 18.6 Hz.
- The metal springs have a loss factor  $\eta = 1/Q$ , corresponding to a spring constant with an imaginary part  $k = \text{Re}(k)(1 + i\eta)$ . The damping layers in the springs contribute  $\eta = 2.5\%$ , and the Fluorel seats contribute an additional  $\eta = 1.5\%$ , for a total  $(4 \pm 1)\%$ .
- Each stage has a simple pole transfer function,  $T_i = f_i^2 / (f_i^2 - f^2 + i f_i^2 / Q_i)$ , with  $Q = 1/\eta$ .

- The stack transfer function is the product:  $T_1T_2T_3T_4$ .
- Then we have the pendulum transfer function, a simple pole with  $f = 0.74$  Hz and  $Q = 3$ .
- Then we have the seismic spectrum itself. I don't know the spectrum at the 40m site (do you? We will measure it!). I use the "Hanford site noisy, w/ microseismic peak", and MULTIPLY BY 10.
- Over short distances, the seismic motions of two or more mirrors are correlated, so that they cancel out when measuring  $L_+$  and  $L_-$ . The correlations are described by Bessel functions, and they require knowledge of the seismic wave velocity spectrum. Using a Matlab file from Nergis, I determined a suppression factor  $S_{corr}(f)$  to account for this effect. For the 38.5 m arm length, we get  $S(f) = (f/4)^{1.25}$  below  $f = 4$  Hz, then  $S(f) = 1$ .
- The product of these spectra give the curves shown in the figures,

$$T_{zz}(f) = T_1(f)T_2(f)T_3(f)T_4(f);$$

$$x_{mirr}(f) = x_{seis}(f)T_{zz}(f)T_{pend}(f)S_{corr}(f).$$

## 5.1 The modelled transfer function

The stacks are designed and modelled as described in the appendix. Here we focus only on the three-legged stacks housing the core optical components; the input and output chamber stacks have similar properties and less critical requirements.

The vertical transfer function  $T_{zz}$  is shown in Fig. 3, and the vertical motion at the top of the stack,  $z_{top}(f)$ , is shown in Fig. 4. In both figures, we show the stacks with all viton springs, all damped metal springs, and a mixture.

The features to note are:

- At high frequencies, all the stack transfer functions have the expected  $f^{-8}$  falloff.
- The metal stacks have superior isolation at higher frequencies compared with the viton, with the mixed stacks lying in between. The frequency at which the vertical displacement falls below  $1^{-18}$  m/ $\sqrt{\text{Hz}}$  is 39 Hz for metal and 91 Hz for viton.
- The metal stacks have resonant peaks that are less damped and at lower frequencies than the viton stacks, leading to higher peak motion at the resonant frequencies. The viton peaks are all but washed out by the damping.

The numbers used for the springs, all of which probably require confirmation, are summarized in table 1.

The numbers for the stacks are summarized in tables 2 through 5. Analogous tables for LIGO stacks appear in Ref. [4], and we have checked our calculations against all the numbers in those tables.

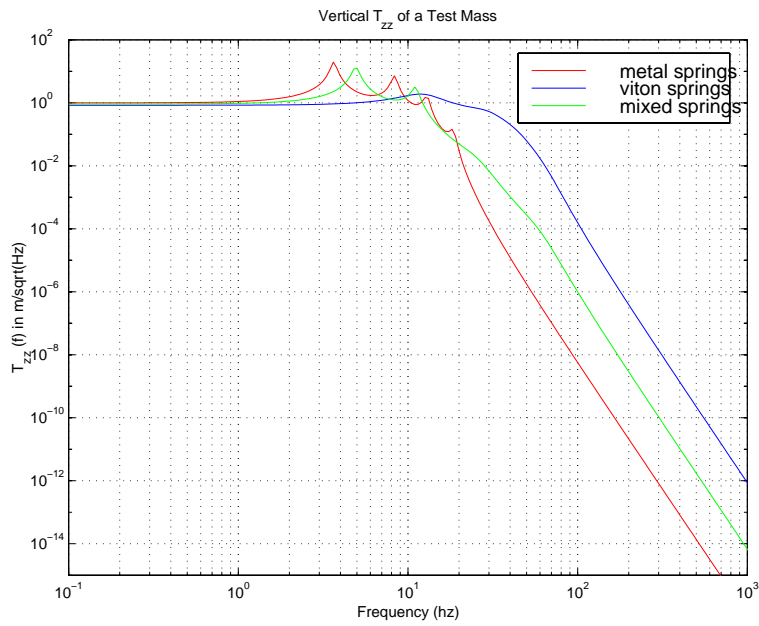


Figure 3: Vertical transfer function  $T_{zz}$  (predicted) for 40m seismic stacks built with damped metal springs, viton springs, or a mixture.

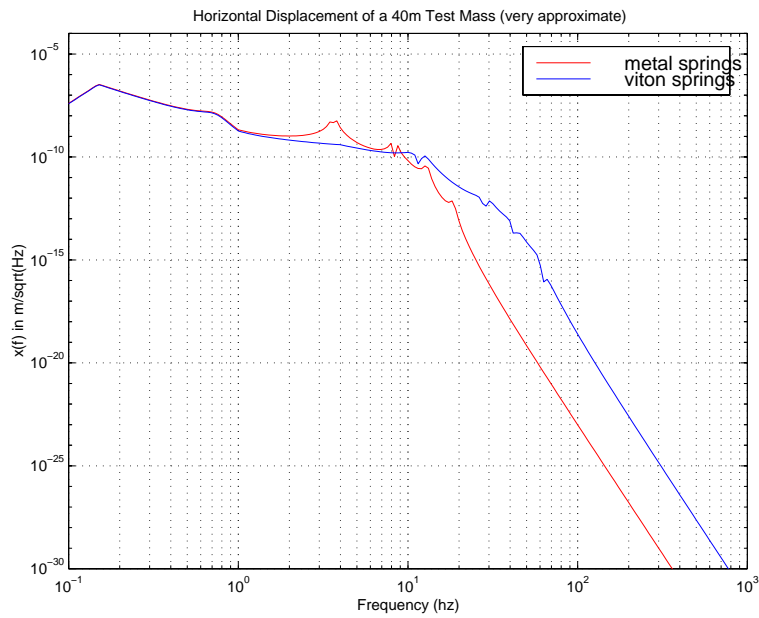


Figure 4: Vertical motion  $z(f)$  (predicted) for 40m seismic stacks built with damped metal springs, viton springs, or a mixture.

Table 1: Spring parameters.

| Spring:              | damped metal | viton  |
|----------------------|--------------|--------|
| $k$ at 100 Hz (Nt/m) | 66317        | 832400 |
| $P_{max}$ (kg)       | 45           | 57     |
| $\eta$ (%)           | 4            | 30     |
| $Q$                  | 25           | 3.3    |

Table 2: Stack parameters for 40m three-legged stacks with damped metal springs. The masses and cumulative masses are for the entire stage, summing all three legs. The number of springs  $n_{springs}$  is fixed to an integral multiple of 3. The ratio of the actual load to the maximal load borne by the springs is  $P_{load}/P_{max}$ . The resonant frequencies of each stage,  $f_{stage}$ , is given assuming no couplings between stages, and  $f_{norm}$  is from a normal mode analysis of those couplings.

| Stage   | mass (kg) | cum mass (kg) | $n_{springs}$ | $P_{load}/P_{max}$ (%) | $f_{stage}$ (Hz) | $f_{norm}$ (Hz) |
|---------|-----------|---------------|---------------|------------------------|------------------|-----------------|
| Payload | 50        | 50            |               |                        |                  |                 |
| 4 (top) | 173       | 223           | 6             | 66                     | 6.7              | 3.6             |
| 3       | 275       | 498           | 12            | 73                     | 8.6              | 8.3             |
| 2       | 275       | 773           | 18            | 76                     | 10.5             | 13.0            |
| 1 (bot) | 275       | 1048          | 24            | 77                     | 12.1             | 18.6            |

Total springs/stack = 60.  
 $\log_{10}(T_{zz})$  at 100 Hz = -8.25.

## 5.2 Mixed stack

The “mixed” stack has viton springs in the upper (or lower) two stages, with metal springs in the remaining stages. The mixture was investigated in the hope of finding a solution with intermediate performance at all frequencies, as a compromise between the advantages and disadvantages of the all-metal design. Unfortunately, that hope was not realized.

The mixed stack performance lies in between the two extreme cases, at falloff frequencies, and has resonant peak frequencies that lie in between as well.

However, whether the viton is put at the top or the bottom of the mixed stack, the lowest peak frequencies are the least damped, because they are dominated by the less stiff metal springs.

Thus, although a mixed stack can permit some tuning of the falloff frequency behavior and resonant peak frequencies, it provides little help in damping the overall rms motion.

As far as contamination is concerned, the amount of viton used can be kept to a minimum, in a hybrid stack, by using viton in the top two stages.

## 5.3 RMS motion

We calculated the total (rms) motion  $z_{rms}$  and  $v_{rms}$  from a minimum frequency  $f_{min}$  to a maximum (in this case,  $f_{max} = 4$  kHz, but it doesn’t matter, since the motions are all negligible at high frequencies).

Table 3: Stack parameters for 40m three-legged stacks with viton springs, according to these calculations (the reality is to be determined upon disassembly, since we can't find original specifications). The masses and cumulative masses are for the entire stage, summing all three legs. The number of springs  $n_{springs}$  is fixed to an integral multiple of 3. The ratio of the actual load to the maximal load borne by the springs is  $P_{load}/P_{max}$ . The resonant frequencies of each stage,  $f_{stage}$ , is given assuming no couplings between stages, and  $f_{norm}$  is from a normal mode analysis of those couplings.

| Stage   | mass (kg) | cum mass (kg) | $n_{springs}$ | $P_{load}/P_{max}$ (%) | $f_{stage}$ (Hz) | $f_{norm}$ (Hz) |
|---------|-----------|---------------|---------------|------------------------|------------------|-----------------|
| Payload | 50        | 50            |               |                        |                  |                 |
| 4 (top) | 173       | 223           | 6             | 66                     | 24.1             | 12.0            |
| 3       | 275       | 498           | 9             | 98                     | 26.5             | 28.9            |
| 2       | 275       | 773           | 15            | 91                     | 34.3             | 42.4            |
| 1 (bot) | 275       | 1048          | 21            | 88                     | 40.6             | 60.7            |

Total springs/stack = 51.  
 $\log_{10}(T_{zz})$  at 100 Hz = -3.80.

Table 4: Stack parameters for 40m one-legged small chamber stacks with damped metal springs.

| Stage   | mass (kg) | cum mass (kg) | $n_{springs}$ | $P_{load}/P_{max}$ (%) | $f_{stage}$ (Hz) | $f_{norm}$ (Hz) |
|---------|-----------|---------------|---------------|------------------------|------------------|-----------------|
| Payload | 50        | 50            |               |                        |                  |                 |
| 4 (top) | 68        | 118           | 3             | 87                     | 6.5              | 3.6             |
| 3       | 145       | 263           | 6             | 97                     | 8.4              | 8.2             |
| 2       | 145       | 407           | 9             | 99                     | 10.2             | 12.8            |
| 1 (bot) | 145       | 552           | 13            | 94                     | 12.3             | 18.3            |

Total springs/stack = 31.  
 $\log_{10}(T_{zz})$  at 100 Hz = -8.30.

Table 5: Stack parameters for 40m one-legged small chamber stacks with viton springs, according to these calculations (the reality is to be determined upon disassembly, since we can't find original specifications).

| Stage   | mass (kg) | cum mass (kg) | $n_{springs}$ | $P_{load}/P_{max}$ (%) | $f_{stage}$ (Hz) | $f_{norm}$ (Hz) |
|---------|-----------|---------------|---------------|------------------------|------------------|-----------------|
| Payload | 50        | 50            |               |                        |                  |                 |
| 4 (top) | 68        | 118           | 3             | 69                     | 23.4             | 11.9            |
| 3       | 145       | 263           | 5             | 93                     | 27.3             | 28.1            |
| 2       | 145       | 407           | 8             | 90                     | 34.5             | 42.2            |
| 1 (bot) | 145       | 552           | 10            | 97                     | 38.6             | 60.4            |

Total springs/stack = 26.  
 $\log_{10}(T_{zz})$  at 100 Hz = -3.84.

Table 6: RMS vertical motion, from  $f_{min} = 0.1$  Hz to  $f_{max} = 4$  kHz.

| Spring:                           | damped metal | viton | mixed |
|-----------------------------------|--------------|-------|-------|
| $z_{rms}$ ( $\times 10^{-8}$ m)   | 5.00         | 4.20  | 4.58  |
| $v_{rms}$ ( $\times 10^{-8}$ m/s) | 9.41         | 5.50  | 7.70  |

What value of  $f_{min}$  should we choose? This is a subtle question, depending on the details of the feedback control mechanism.

These integrals will be dominated by the low frequency region. We see from Fig. 4 above that the motion of the damped metal and viton stacks are basically identical below 1 Hz, including in the region of the 0.15 Hz microseismic peak.

Below 0.1 Hz, the correlations in the seismic motion of the mirrors suppresses the differential motion, but the seismic spectrum is large there.

For definiteness, Table 6 uses  $f_{min} = 0.1$  Hz.

## 5.4 Summary

Clearly, metal springs deliver the best seismic isolation at signal frequencies, but have poorly-damped resonant peaks and relatively larger rms motions at frequencies from 1 to 20 Hz.

Does the relatively larger rms motions of the mirrors on damped metal spring stacks make the difference between a functional control system and a dysfunctional one?

Combining this question with the questions regarding contamination, and the considerable effort required to rebuild the stacks and bake out the vacuum envelope, what shall we do?

## 6 Task-list for 40m bake-out.

### 6.1 At end of Michigan experiment (11/99)

- Catalog (on computer) all detector equipment, both inside and outside of vacuum envelope. Determine disposition: re-use, ship elsewhere, store clean, store “dirty”, etc. Find a semi-permanent storage place for surplus equipment! (Ugolini, done).
- Preclean accumulated surplus equipment from 40m: Coherent lasers, various unused parts (Vass)
- Find and assemble all existing drawings of vacuum chambers, stacks, other vacuum elements. Ideally, in electronic form. Update and annotate, and submit to DCC. (Vass, Althouse, Craig Conley. Done?).
- Build new vacuum control system, using existing pumps, gauges, valves.
  - Hardware/software interface: VME crate, CPU, SADCs, BIOS, SDACs. (Heefner, Bork, Weinstein, etc)
  - Wiring to new hardware/software interface. (Heefner, Bork, Vass, Ted Jou)
  - EPICS software: Data base, state machine, GUI. (Ted Jou, Weinstein, Heefner, Bork).
  - Operational modes: protected, unprotected, fully automatic

- Test everything, offline, not connected to hardware. (Ted Jou, Ugolini, Weinstein, Heefner, Bork; in progress).
- Procure 5 computer-controlled pneumatic gate valves (clean) for ion pumps, pressure-interlocked to  $10^{-6}$  torr. (Vass; in progress).
- Select heater jackets from LIGO chamber bakeout. Make use of their controllers and associated equipment, operating with existing lab 480V power. Bring all that equipment to Caltech, and test. (Vacuum engineer, Vass).
- Design a system for jacking up the entire vacuum system by 6in, to permit heating jackets under the chambers. Procure all necessary equipment. (Vacuum engineer, Vass).
- Procure new optical table for output chamber (Asiri, Conley).
- Design and build seismic stack for output chamber (Asiri, Conley).
- Receive and validate (bake and RGA screen) new metal springs and fluorel seats. (Asiri, Conley).
- Update calibration leaks to LIGO variety (Vass).
- Establish and document vacuum / contaminant level with existing system, under vacuum. (Vass, Ugolini, Weinstein).

## 6.2 During vent ( 11/99 - 3/2000)

- Vent vacuum system. (Vass, Weinstein, Ugolini).
- remove all detector equipment, store. (Vass, Weinstein, Ugolini).
- Remove old 40m test masses, examine under microscope (Vass, Weinstein, Ugolini, Armandula, Camp).
- Measure seismic motion at bottom and top of stacks, determine transfer function, check against model (Vass, Weinstein, Ugolini).
- remove ion pumps, replace with blank plate. (Vass, Weinstein, Ugolini).
- regenerate ion pumps individually with small turbopump. (Vass, Weinstein, Ugolini).
- disassemble stacks, measuring all dimensions and weighing all stack elements. (Vass, Weinstein, Ugolini).
- Zero torsional deflection of bellows on all chambers and test spare one for maximum limit. (Vass, Weinstein, Ugolini).
- Update or create new drawings to correctly represent the stacks, chambers, etc. (Vass, Craig Conley, Asiri).
- Machine new stack elements for one-leg stack for new output chamber. Machine present stack elements & top plates to accomodate metal springs. (Asiri, machinists).

- Install new LIGO-like calibrated leaks.
- Install new dry-clean air purge vent system.
- Install new RGA if needed.
- Connect and commission new vacuum control system; test EPICS control and data logging. (Weinstein, Heefner, Bork, Ugolini).
- Jack up entire vacuum system 3 in (including stack support beams/legs), and place heaters underneath. (Vacuum engineer, Vass, Weinstein, Ugolini).
- Pump down to look for leaks (*e.g.*, in beam tube seams) created by jacking up; repair if needed. (Vacuum engineer, Vass, Weinstein, Ugolini).
- RGA analysis of empty vacuum chamber with support beams and plates to establish baseline. (Vass, Weinstein, Ugolini).
- Assemble and install new output chamber. (Vass, Weinstein, Ugolini, Asiri).
- Wrap entire vacuum system with heating jackets, connect all controllers, instrumentation. (Vacuum engineer, Vass, Weinstein, Ugolini).
- Place all stack elements, optical tables, ion pump/gate valve assemblies, (springs? detector elements?) in a heater jacket on the floor (OR send to commercial vendor for cleaning and baking). (Vacuum engineer, Vass, Weinstein, Ugolini).

### 6.3 Bake-out (3/2000)

- Bake for 2-4 weeks, monitoring everything, logging to disk/tape, documenting everything. (Vacuum engineer, Vass, Weinstein, Ugolini).
- Document state of vacuum / contaminants. (Vass, Weinstein, Ugolini).
- Disassemble, remove, and store bake-out jackets, controllers, and other equipment. (Vacuum engineer, Vass, Weinstein, Ugolini).
- Vent system with clean, dry air. (Vass, Weinstein, Ugolini).
- Assemble all stacks and optical tables, measuring and documenting all dimensions. (Vass, Weinstein, Ugolini).
- Install ion pumps and gate valves, connect to new vacuum control system.
- Seal and pump down vacuum system, commission ion pumps. Maintain vacuum until ready for detector installation. (Vass, Weinstein, Ugolini).

## 6.4 COSTS

- Manpower (Vass, Conley, Ugolini, etc).
- Electrician to connect/disconnect 480V.
- Gate valves for ion pumps.
- VME-based control system (crate, cpu, modules, cables).
- Misc control hardware.
- Clean air purge system (\$20K).
- LIGO-like calibrated leaks (\$5K?).
- New LIGO-like RGA to replace old 40m one? (\$30K?)
- Heater jackets & controllers for ion pump regeneration.
- New optical table.
- Metal springs and seats (\$53.6K).
- New stack elements, remachine existing stack elements (\$30K?).
- Packing & shipping heater jackets and controller (\$10K?).

## 7 Acknowledgements

Many thanks to Bill Althouse and Jordan Camp.

## References

- [1] LIGO drawing D961304-06: [http://www.ligo.caltech.edu/LIGO\\_web/dcc/docs/D961304-06.pdf](http://www.ligo.caltech.edu/LIGO_web/dcc/docs/D961304-06.pdf) .
- [2] LIGO note M960115-00, [http://www.ligo.caltech.edu/LIGO\\_web/dcc/docs/M960115-00.pdf](http://www.ligo.caltech.edu/LIGO_web/dcc/docs/M960115-00.pdf) .
- [3] LIGO drawings 1205425-1205429, 1205431-1205433, 1205435-1205439, 1205441-1205452, 1202092, 1101012.
- [4] E. Ponslet, HYTEC-TN-LIGO-01 (1996); HYTEC-TN-LIGO-02 (1996); HYTEC-TN-LIGO-03 (1996); HYTEC-TN-LIGO-04a (1996); HYTEC-TN-LIGO-07a (1997);
- [5] LIGO note M970104-00, [http://www.ligo.caltech.edu/LIGO\\_web/dcc/docs/M970104-00.pdf](http://www.ligo.caltech.edu/LIGO_web/dcc/docs/M970104-00.pdf) .
- [6] A. Abramovici, T.T. Lyons, F.J. Raab, Appl. Opt. 34, 183 (1995).
- [7] J. Camp, LIGO G990016-00-D (<http://docuserv.ligo.caltech.edu/docs/public/G/G990016-00.pdf>); J. Camp, D. Coyne, and D. Li, Appl. Opt. 38, 5378 (1999), LIGO P990032-00-D.
- [8] J. Giaime, PhD thesis, MIT (1995); J. Giaime, P. Saha, D. Shoemaker, and L. Sievers, Rev. Sci. Instrum. 67, 208-214 (1996).